ACS APPLIED MATERIALS & INTERFACES

Research Article

www.acsami.org

Effects of Nonequilibrium Growth, Nonstoichiometry, and Film Orientation on the Metal-to-Insulator Transition in $NdNiO_3$ Thin Films

Eric Breckenfeld,[†] Zuhuang Chen,[‡] Anoop. R. Damodaran,[‡] and Lane W. Martin*[,‡,§]

[†]Materials Science and Technology Division, Code 6364, Naval Research Laboratory, Washington, DC 20475, United States
[‡]Department of Materials Science and Engineering, University of California, Berkeley, Berkeley, California 94720, United States
[§]Materials Science Division, Lawrence Berkeley National Laboratory, Berkeley, California 94720, United States

Supporting Information

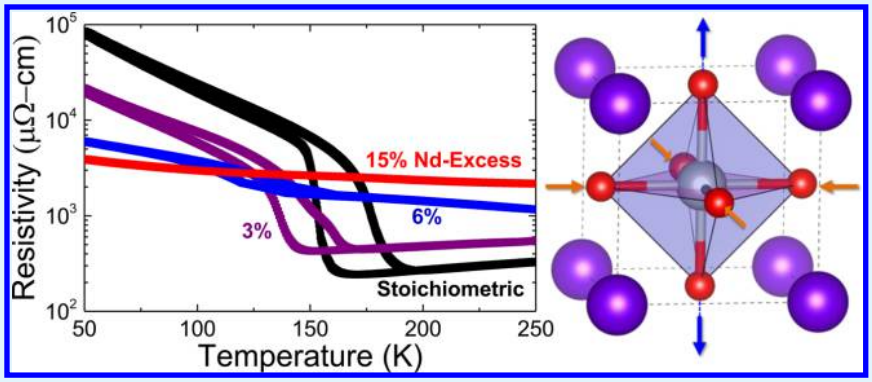

ABSTRACT: Next-generation devices will rely on exotic functional properties not found in traditional systems. One class of materials of particular interest for applications are those possessing metal-to-insulator transitions (MITs). In this work, we probe the relationship between variations in the growth process, subsequent variations in cation stoichiometry, and the MIT in $NdNiO_3$ thin films. Slight variations in the growth conditions, in particular the laser fluence, during pulsed-laser deposition growth of $NdNiO_3$ produces films that are both single-phase and coherently strained to a range of substrates despite possessing as much as 15% Nd-excess. Subsequent study of the temperature-dependence of the electronic transport reveals dramatic changes in both the onset and magnitude of the resistivity change at the MIT with increasing cation nonstoichiometry giving rise to a decrease (and ultimately a suppression) of the transition and the magnitude of the resistivity change. From there, the electronic transport of nearly ideal $NdNiO_3$ thin films are studied as a function of epitaxial strain, thickness, and orientation. Overall, transitioning from tensile to compressive strain results in a systematic reduction of the onset and magnitude of the resistivity change across the MIT, thinner films are found to possess sharper MITs with larger changes in the resistivity at the transition, and (001)-oriented films exhibit sharper and larger MITs as compared to (110)- and (111)-oriented films as a result of highly anisotropic in-plane transport in the latter.

KEYWORDS: *nickelates, epitaxial thin films, stoichiometry, strain, transport*

INTRODUCTION

The electronic structure and properties of conducting metal oxides have been a widely investigated topic for many decades because of the exotic phenomena found in these systems.[1] For instance, materials possessing metal−insulator transitions (MITs) have been particularly appealing because of their complex materials physics and potential for applications.[2,3] Recently, there has been increasing interest in rare-earth nickelates due to their sharp, temperature-driven, first-order MIT.[4] The rare-earth nickelates possess the chemical formula $RNiO_3$, where R is from the lanthanide series of rare earth elements. It has been observed that the onset temperature of the MIT (T_{MI}) scales inversely with the ionic radius of the rare-earth cation with La, the largest ionic radius, resulting in metallic behavior at all temperatures,[4] and Lu, the smallest ionic radius, possessing the highest $T_{MI} \approx 600$ K.[4] Antiferromagnetic ordering has also been observed (except in $LaNiO_3$), the onset of which either corresponds to the MIT (for $PrNiO_3$ and $NdNiO_3$) or occurs at a lower temperature than T_{MI} (for the remaining $RNiO_3$ systems).[5] We note that there exists a deeply complex interplay between the octahedral structure (i.e., bond lengths, angles, rotations, etc.) and the electrical and magnetic properties and that even small structural distortions can induce significant changes in T_{MI} or the magnetic T_N.[6] Among other applications, this class of materials has been considered for sensors,[4] electronic switches,[7] thermochromic coatings,[8] and nonvolatile memories.[3]

Received: September 19, 2014
Accepted: November 14, 2014
Published: November 14, 2014

A number of studies have been performed on both bulk and thin-film samples to study the origin and nature of conductivity in the nickelates.[7,9−12] These studies have probed chemical doping,[13] hydrostatic pressure,[9,10] and epitaxial strain[11,12] as possible routes to modify T_{MI} and the character of the MIT by manipulating the angle and spacing of the Ni−O−Ni bond and, in the case of chemical doping, by carrier injection. For instance, using divalent and tetravalent cations (including Ca^{2+}, Sr^{2+}, Ce^{4+}, and Th^{4+}) as substitutions for the R^{3+} cation has allowed researchers to explore both electron and hole doping for the nickelate system. In general, carrier doping has a tendency to lower the T_{MI} and damp the magnitude of the transition; with hole doping causing more significant damping than electron doping. One limitation of using chemical doping to effect change on the nature of the MIT is that it is difficult to separate the electronic and strain-related effects that arise from substituting differently sized cations into the lattice. To separate out this factor, others have used top gates to drive charge into or out of the film.[7] These studies have seen similar results, with a general suppression of the T_{MI}.

Studies on strain effects generally fall into one of two categories: (1) application of large hydrostatic pressures and (2) epitaxial thin-film strain studies. Hydrostatic pressure studies have universally observed a decrease in the T_{MI} with increasing pressure.[9,10] The results of experiments on epitaxial strain have been somewhat less consistent and, in some cases, contradictory. For example, in $NdNiO_3$, compressive strain has been seen to increase,[11] decrease,[7] or even completely suppress[12] the T_{MI}. Even from a theoretical approach, researchers have had difficulty in determining how the Ni−O−Ni bonds (i.e., the bond angle and distance) will respond to epitaxial strain and, in turn, impact the properties.[14] For compressive strain, it has been suggested that either an enhanced rotation of the oxygen octahedra (resulting in an increase of T_{MI}) or a decrease in the Ni−O bond distance and a straightening of the Ni−O−Ni bond angle (resulting in a decrease of T_{MI}) could be possible.[14] Still other reports have argued that in-plane strain anisotropy is the most important factor, instead of simply the value and sign of the applied strain.[15] A number of first-principles studies have also been performed for the rare earth nickelates and suggest that the symmetry of the underlying substrate[16] has an additional impact on the rotation and shape of the oxygen octahedra, which is responsible for some of the observed differences in the transport profiles. All told, despite extensive studies, there is no general agreement on the interaction between epitaxial strain and transport properties in rare earth nickelate thin films.

The complexity of the situation in films can be further exacerbated by the fact that film stoichiometry, including cation and anion chemistry, can also potentially play a role in the evolution of both structure and properties. Many reports have studied or alluded to the role of oxygen nonstoichiometry[10,14,17−19] to account for discrepancies in reported transport data. Cation nonstoichiometry, however, has been largely ignored with few groups including compositional studies as part of their growth process. Recent work, however, indicates that control over cation stoichiometry is a nontrivial issue, especially for films produced via the most common methods in research and development (including pulsed-laser deposition).[20−27] Most studies use only X-ray diffraction to probe phase-purity,[28,29] but such an approach has been shown to be insufficient to accurately assess the chemical state of such complex oxides. It is well-known that the perovskites can remain "phase pure" and exhibit diffraction patterns consistent with what might be expected, despite possessing many atomic-percent of nonstoichiometry. Although X-ray diffraction can highlight some telltale signs of nonstoichiometry, such as lattice expansion, extensive studies coupling lattice expansion with chemistry and the associated transport behavior in the nickelates have not been completed. With this in mind, and with a knowledge that many factors, including cation-doping, pressure, epitaxial strain, and so on, can drive dramatic changes in the nature of electronic transport in the nickelate systems, it seems important to assess the role of nonstoichiometry as well. Growing evidence has suggested that even a slight deviation in chemistry can drive a dramatic change of transport properties in conducting oxide systems[30−33] and thus motivates the current study.

In this work, we undertook a detailed study of the relationship between variations in the growth process, subsequent variations in cation stoichiometry, and ultimately the electronic properties of $NdNiO_3$ thin films. We reveal that by changing the growth conditions, in particular the laser fluence, during pulsed-laser deposition growth of $NdNiO_3$, we can produce films that are, from X-ray diffraction, single-phase despite possessing as much as 15% Nd-excess. For thicknesses <70 nm, regardless of stoichiometry, the films remain coherently strained on a wide range of perovskite substrates. Subsequent study of the temperature-dependence of the electronic transport, however, reveals dramatic changes in both the T_{MI} and the magnitude of the resistivity change at the MIT. In general, increasing cation nonstoichiometry gives rise to a decrease (and ultimately a suppression) of the T_{MI} and the magnitude of the resistivity change associated with the MIT. Armed with the ability to produce nearly stoichiometric $NdNiO_3$ thin films, we proceed to explore epitaxial strain, thickness, and orientation-dependence of the temperature-dependent electronic transport. As the lattice mismatch transitions from tensile to compressive in nature, we observe a systematic reduction of T_{MI} and a corresponding reduction in the magnitude of the resistivity change across the MIT. In general, thinner films are found to possess sharper MITs with larger changes in the resistivity across the MIT. Finally, studies of film orientation reveal that (001)-oriented films possess both the sharpest and largest change in resistivity associated with the MIT as compared to the (110)- and (111)-oriented films. The smearing of the MIT in the (110)- and (111)-oriented films is found to arise from highly anisotropic transport properties along the in-plane directions of the film, which can give rise to changes in the T_{MI} along different directions as large as ∼60 K and differences in the resistance change below T_{MI} as large as 500%. These variations are connected to the anisotropic strain that is applied to the material.

EXPERIMENTAL SECTION

We grew 10−120 nm thick $NdNiO_3$ (which possesses an orthorhombic structure with lattice parameters a = 5.389 Å, b = 5.382 Å, and c = 7.610 Å and a pseudocubic lattice parameter a_{pc} = 3.807 Å) thin films on $LaAlO_3$ (001), (110), and (111) (cubic, a = 3.79 Å), $0.3(LaAlO_3)−0.7(Sr_2AlTaO_6)$ (LSAT) (001) (cubic, a = 3.87 Å), $NdGaO_3$ (110) (orthorhombic, a = 5.433 Å, b = 5.503 Å, and c = 7.716 Å; a_{pc} = 3.86 Å), and $SrTiO_3$ (001) (cubic, a = 3.905 Å) single-crystal substrates. The films were grown via pulsed-laser deposition using a KrF excimer laser (LPX 305, Coherent) in 200 mTorr of O_2 at a frequency of 5 Hz at 750 °C (measured by a thermocouple embedded in the heater block; samples attached via Ag paint). A ceramic, stoichiometric $NdNiO_3$ target was used for all growths. The

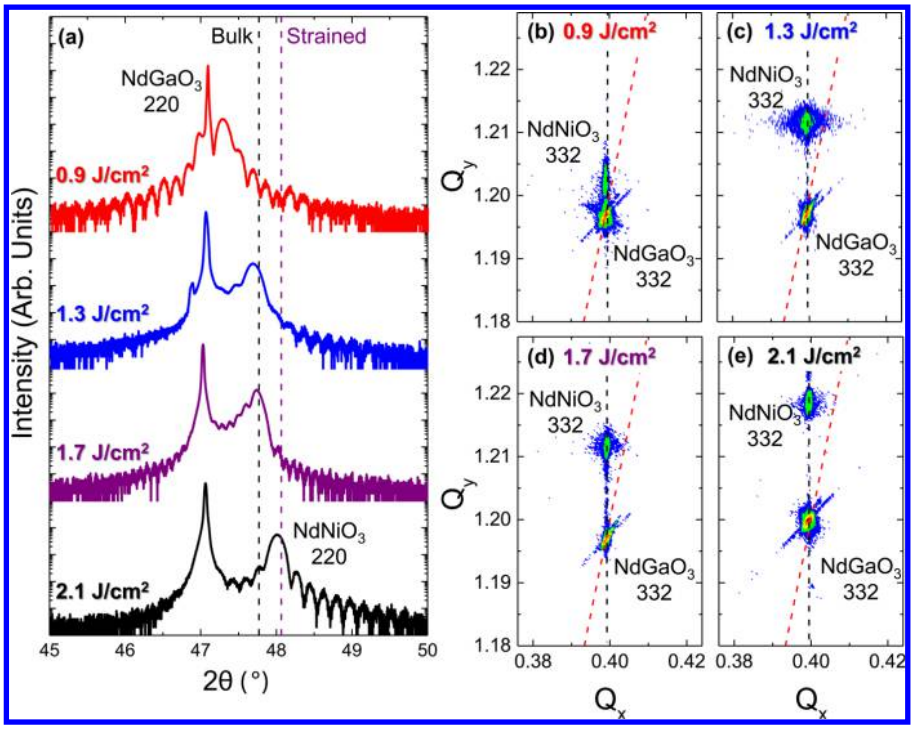

Figure 1. (a) $\theta-2\theta$ X-ray diffraction patterns about the 220-diffraction conditions of the $NdNiO_3$ film and $NdGaO_3$ substrate, respectively. Films are single-phase, of high-quality (exhibiting Laue fringes), and show a systematic variation in the out-of-plane lattice parameter of the $NdNiO_3$ film as a function of laser fluence during growth. X-ray reciprocal space mapping studies about the 332-diffraction condition of the film and substrate for films grown at a laser fluence of (b) 0.9, (c) 1.3, (d) 1.7, and (e) 2.1 J/cm^2. In all cases, the films and substrates reveal the same in-place lattice parameter (i.e., Q_x-value) indicating that all films are coherently strained to the substrate.

growths were completed in an on-axis geometry with a 6.35 cm target-to-substrate spacing. Following growth, films were cooled at 5 °C/min to room temperature in 700 Torr of oxygen to promote oxidation. As part of this work, we focused on the role of changing laser fluence on the evolution of the structure and properties of the $NdNiO_3$ thin films. We have explored laser fluences ranging from 0.5 to 2.1 J/cm^2 (details of the laser fluence determination are provided in the Supporting Information).

Following growth, the films were subjected to extensive structural, chemical, and property studies. The structure of the $NdNiO_3$ films was studied using X-ray diffraction $\theta-2\theta$ and reciprocal space mapping studies (Panalytical, X'Pert MRD Pro), the as-grown film stoichiometry was probed using Rutherford backscattering spectrometry (RBS), and the temperature-dependent electronic transport studies were completed in a van der Pauw configuration in a Quantum Design PPMS (resistance mode, excitation current of 99 μA).

RESULTS AND DISCUSSION

We begin by examining the structure of the $NdNiO_3$ films as determined by X-ray diffraction studies. For brevity, we focus here on the evolution of structure in 70 nm $NdNiO_3/NdGaO_3$ (110) heterostructures as an illustrative example. X-ray diffraction $\theta-2\theta$ studies reveal that the films grown at laser fluences of 0.9 J/cm^2 and higher are single-phase (Supporting Information, Figure S1a) with films grown at lower fluences showing the presence of parasitic, Nd-rich phases Nd_2NiO_4 and $Nd_4Ni_3O_8$ (which belong to the $A_{n+1}B_nO_{2n+2}$ series, which is related to, but distinct from, the Ruddlesden–Popper series;[34] Supporting Information, Figure S1b). Close inspection of the single-phase $NdNiO_3$ films reveals that the out-of-plane lattice parameter of the films gradually contracts as the fluence is increased (Figure 1a and Supporting Information, Figure S1c). From epitaxial strain and Poisson effects, a decrease in the c axis lattice parameter by 0.7% as compared to bulk is expected;[35] however, for the films studied here, an additional expansion of the out-of-plane lattice parameter (from the predicted coherently strained peak position) of 0.2–1.6% is observed as we move from high to low laser fluences. This matches closely with the results observed previously for $SrTiO_3$ films[22−24] and, considering the Nd-rich phases observed at lower fluence, seems to indicate a fluence dependence of the film stoichiometry with lower fluence favoring Nd-excess. The expansion of the out-of-plane lattice parameter is indicative of the presence of lattice-distorting cation defects, likely vacancies or vacancy complexes, which are known to expand the lattice.[36,37] Despite this fact, the quality of the films appears to be quite high, as all films reveal relatively sharp diffraction peaks and clear Laue oscillations, which are indicative of excellent film and interface quality. Similar results have been found for growth on the other substrates, and additional X-ray diffraction $\theta-2\theta$ and reciprocal space mapping studies are provided (Supporting Information, Figure S2).

The in-plane lattice constants and the strain state of the films was investigated by reciprocal space mapping studies about the 332-diffraction conditions of both the $NdNiO_3$ film and the $NdGaO_3$ substrate. Focusing again on the films grown between 0.9 and 2.1 J/cm^2 (Figure 1b-e), the reciprocal space mapping studies reveal that all films, regardless of laser fluence, are coherently strained to the substrate and possess identical in-plane lattice parameters, as indicated by the film and substrate peaks having the same Q_x values. Additionally, consistent with the $\theta-2\theta$ scans, the out-of-plane lattice parameter of the films in the Q_y direction is found to decrease as the laser fluence increases. The combination of the $\theta-2\theta$ and reciprocal space mapping studies indicates that the changes in the out-of-plane lattice parameter are not the result of some complex strain

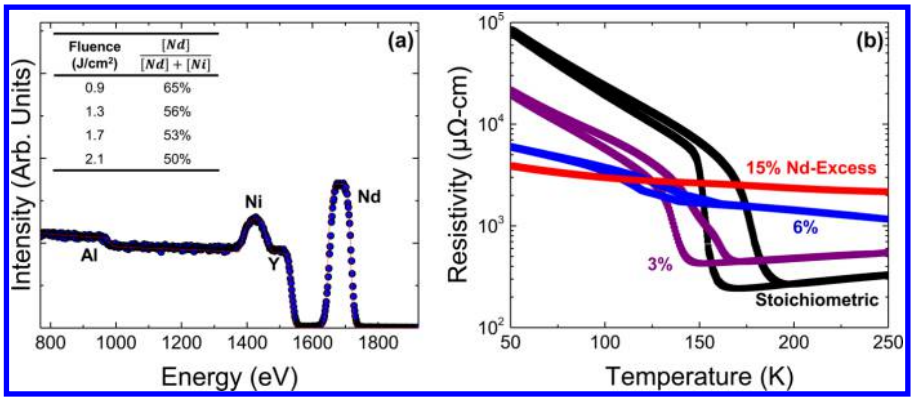

Figure 2. (a, ●) Characteristic Rutherford backscattering spectrometry (RBS) data set and (red line) a corresponding fit to the data for a nearly stoichiometric film grown at 2.1 J/cm^2; (inset) stoichiometry (here, in Nd percentage) as a function of laser fluence. (b) Temperature dependence of the resistivity of $NdNiO_3$ films controlled to possess (black, stoichiometric) 0, (purple) 3, (blue) 6, and (red) 15% Nd-excess showing dramatic dependence of the MIT on film chemistry.

relaxation process in the films, but are indicative of changes in the volume of the unit cell of the $NdNiO_3$, as the growth conditions are varied. Regardless of the laser fluence, the films are found to be coherently strained and this results in a systematic decrease in the out-of-plane lattice parameter as the laser fluence is increased. Based on these structural studies alone, it is clear that the structure of the $NdNiO_3$ films is acutely sensitive to the growth parameters. To determine the cause of the observed structural changes and their ramifications on the MIT behavior, we performed studies of both the film chemistry and physical properties of these films.

A characteristic RBS spectrum for a $NdNiO_3/YAlO_3$ film grown at 2.1 J/cm^2 is provided (Figure 2a). RBS studies focused on films grown on $YAlO_3$ for practical considerations because clear separation of peaks in the spectra simplifies and improves the quality of the compositional analysis. No correlation between substrate selection and chemistry was observed (within the error of the measurement); in other words, regardless of substrate selection, the growth conditions were found to dominate the stoichiometry that was obtained. Consistent with our hypothesis, dramatic variations in the cation chemistry, here reported as a percentage of Nd excess or deficiency as calculated by [Nd]/([Nd] + [Ni]) × 100, are observed as the laser fluence is varied (inset, Figure 2a). We note that we cannot uniquely differentiate between Nd excess and Ni deficiency, but for simplicity, we refer to the chemical state in terms of the Nd content. By comparing our experimental data to multiple calculated fits, we have determined that the accuracy of our compositional data is ±0.7% (a more in-depth determination of the error of the RBS studies is provided in the Supporting Information, Figure S3). Stoichiometric films, within the error of the RBS studies, are found to be produced at relatively high laser fluences (2.1 J/cm^2). Upon decreasing the laser fluence, the films trend toward more and more Nd excess and when one reaches a laser fluence of 0.9 J/cm^2 a single-phase, epitaxial, high-quality thin film of 15% Nd excess $NdNiO_3$ is observed. Such trends in cation nonstoichiometry are consistent with results from the growth of both $SrTiO_3$ and $LaAlO_3$,[23,24,30] where lower laser fluence tended to favor excess of the *A*-site cation, and higher laser fluence tended to favor excess of the *B*-site cation. Such effects also help explain the observed lattice distortion (Figure 1 and Supporting Information, Figure S1c), as we observe increasing Nd content to produce an increasing out-of-plane lattice parameter. Again, we would like to reemphasize the fact that these films grown at 0.9 J/cm^2, despite possessing 15% Nd-excess, exhibited no signatures of secondary phases in the X-ray diffraction studies (Supporting Information, Figure S1a). Somewhat surprisingly, this indicates that 15% Nd excess is either within the effective solubility limit (given the kinetic and epitaxial constraints on the system) or that the fraction of any Nd-excess phases are below the sensitivity of the diffraction experiments. These results are crucial because they show that observing single-phase, epitaxial, high-quality diffraction peaks, even those possessing telltale signs of high-quality (i.e., sharp peaks, Laue oscillations), is insufficient evidence of a stoichiometric or "ideal" film. Armed with this information, we determined the impact that the observed deviations in film stoichiometry have on the electronic transport properties.

The resulting temperature-dependent electronic transport profiles for 70 nm thick stoichiometric 3, 6, and 15% Nd-excess films are provided (Figure 2b). Stoichiometric films (black data, Figure 2b) exhibit a sharp MIT whereby the resistivity increases by 2000% over a 15 K wide temperature range about the transition (the onset of which occurs at ∼161 K). Below the phase transition, the resistivity further increases by another 1.5 orders of magnitude by the time the temperature reaches 50 K. Overall, the system shows a 34 000% change in resistivity within the range of temperatures (50−250 K) probed here. This behavior is (roughly) consistent with prior studies of epitaxially strained $NdNiO_3/NdGaO_3$ (110) heterostructures.[7] Upon deviation from stoichiometry and the introduction of Nd excess, we observe an increase (decrease) in the resistivity of the metallic (insulating) states, resulting in a systematic damping of the magnitude of the resistivity changes associated with the MIT, a reduction in the T_{MI}, and a broadening of the transition region in temperature. Even just 3% Nd excess in the films (purple data, Figure 2b) results in a suppression of the exhibited T_{MI} (∼144 K) and a reduction of the resistivity change across the MIT (a 500% increase in resistivity over a 17 K wide temperature range) and only a 4800% change in resistivity across the entire temperature range studied. For films possessing >6% Nd excess (blue and red data are for 6 and 15% Nd excess, respectively, Figure 2b), the films exhibit a semiconducting-like temperature-dependence of resistivity across all temperature ranges probed. Weak or unresolvable MITs are observed in films in this stoichiometry range. For the 6% Nd-excess film, a weak hysteresis is observed between 80

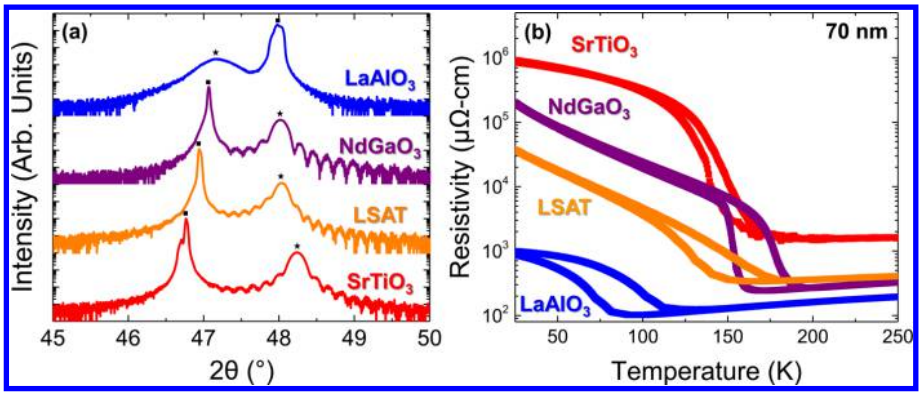

Figure 3. (a) $\theta-2\theta$ X-ray diffraction patterns about the 002 or 220-diffraction conditions of the (blue) $LaAlO_3$, (purple) $NdGaO_3$, (orange) LSAT, and (red) $SrTiO_3$ substrates; (■) substrate peak and (★) film peak. Note the systematic variation in the film peak position with substrate. (b) Corresponding temperature-dependence of resistivity for the various $NdNiO_3$ films grown on the different substrates. Again, the change in substrate strain and symmetry has a dramatic impact on the resulting nature of the MIT.

and 160 K. Overall, the 6 and 15% Nd-excess films exhibit only 500 and 180% changes in resistivity across the entire temperature range studied.

There are several important points to make in summarizing these findings. First, we have shown that cation stoichiometry is a pivotal parameter for controlling the character of the MIT in $NdNiO_3$ films. Second, by using laser fluence to tune the cation stoichiometry of the system, we have managed to fabricate films with different T_{MI} values on the same substrate. This indicates that without carefully controlling the growth process, it is difficult to know whether observed changes in $NdNiO_3$ transport properties are purely the result of substrate-strain-induced effects. It is instead possible that a non-negligible percentage of experimental observations for the $NdNiO_3$ system have probed defect-induced, extrinsic effects. Finally, even though the $NdNiO_3$ phase is capable of handling up to 15% Nd-excess, the transport properties of such films deviate substantially from those of the stoichiometric samples. For this reason, phase purity is a necessary but insufficient condition for achieving sharp, first-order MIT properties. These insights may be instrumental in clearing up some of the experimental inconsistencies in prior works on epitaxially strained $RNiO_3$ films.[7,11,12]

As we attempt to understand the behavior that we have observed, it is illustrative to compare these results to effects observed in both electronic gating and chemical alloying studies of $NdNiO_3$. Upon application of voltages using an ionic liquid contact, researchers observed a reduction of the T_{MI} (~45 K for application for 4 V) and a reduction in the resistivity change associated with the MIT as the applied electric field drives an increase in the carrier concentration and stabilizes the metallic state of the material.[7] Likewise, by alloying with 5% of either Ca^{2+} or Sr^{2+} (corresponding to the addition of holes) or 5% of Th^{4+} (corresponding to the addition of electrons), researchers have observed a reduction of T_{MI} by as much as ~130 K and a corresponding reduction in the magnitude of the resistivity change across the MIT by upward of 3 orders of magnitude.[13] These seemingly contradictory observations were explained by a combination of size effects from the inclusion of different cations (resulting in a change in Ni−O−Ni bond angle and distance) and the fact that all dopants introduce extra carriers (because it is thought that both electrons and holes can be directly incorporated into the Ni−O bands of such Ni^{3+} compounds). For the films studied here, we demonstrate that it is possible to introduce as much as 15% Nd-excess (likely as point defects) via the growth process while maintaining a single-phase thin film. These excess Nd cations provide two possible mechanisms by which to suppress the T_{MI} and drive a reduction in the magnitude of the resistivity change associated with the MIT. Such point defects generally result in (1) an expansion of the lattice[36,37] and (2) the production of excess charge (assuming the charged defects are not totally compensated by other charged defects), which can both impact the nature of electronic transport. This said, we hypothesize that, in these samples, the majority of the effect potentially arises from structural (not charge) mechanisms for the following reasons. First, the production of free charge carriers as a result of the cation nonstoichiometry likely has less influence (although it cannot be totally neglected) on the system as compared to the massive structural changes observed. Although it is impossible to completely exclude doping effects thus far, the individual and clustered charged point-defects can be readily accommodated electronically by other charged defects without the need for the production of free charge carriers. The lattice expansion observed in the films corresponds to a 0.2−1.6% deviation from ideal, a considerably larger value than the lattice expansion observed in the case of bulk chemical doping which was on the order of ~0.01%.[13] On the other hand, these values are similar to the lattice distortions provided by coherent epitaxial growth on substrates, providing an interesting opportunity for comparison. We believe that this expansion of the lattice, resulting from the presence of the defects induced by the growth process, likely changes the structure of the $NdNiO_3$, in particular the nature of the bond angles, bond lengths, and/or octahedral tilts, and therefore stabilizes the metallic phase to lower temperatures. Thus, we have gone on to grow films with ideal stoichiometry on several single-crystal substrates, offering a variety of strain conditions, in order to compare the response of the MIT to similar values of defect-induced strain and coherent epitaxial strain.

Additional 70 nm thick films were grown on $SrTiO_3$ (2.5% lattice mismatch), LSAT (1.6% lattice mismatch), and $LaAlO_3$ (−0.47% lattice mismatch) substrates to compare to those grown on $NdGaO_3$ (1.3% lattice mismatch). Wide angle X-ray $\theta-2\theta$ and reciprocal space mapping studies (Supporting Information, Figure S2) confirm single phase, coherently strained $NdNiO_3$ films on $NdGaO_3$ and LSAT substrates and (potentially) partially relaxed films on $LaAlO_3$ and $SrTiO_3$ substrates. High-resolution $\theta-2\theta$ studies (Figure 3a) exhibit sharp film peaks with clear Laue fringes for all films except

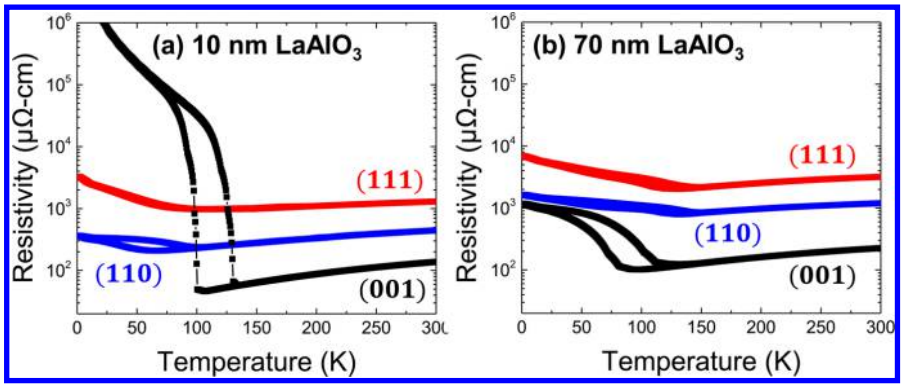

Figure 4. Temperature dependence of resistivity for (a) 10 and (b) 70 nm thick $NdNiO_3$ films grown on (black) (001)-, (blue) (110)-, and (red) (111)-oriented $LaAlO_3$ substrates. Note the dramatic thickness and orientation dependence to the sharpness and magnitude of the MIT.

those grown on $LaAlO_3$. The increased broadness and absence of fringes observed in films grown on $LaAlO_3$ may be a result of the twinned structure and relative poor crystal quality of the substrate and not an indicator that the film is of poor quality. These studies may also indicate that the films grown on $LaAlO_3$ substrates seem to begin relaxing before those on $NdGaO_3$ or LSAT, despite the fact that the magnitude of the strain is smaller for $NdNiO_3$ films on $LaAlO_3$. This can potentially be explained by a number of factors: (1) the poor quality and twinned structure of the $LaAlO_3$ substrates could be causing broadening of the diffraction peak in Q_x space, which could be interpreted as partial relaxation; (2) compressive and tensile strains (as is the case for films on $LaAlO_3$ and $NdGaO_3$ or LSAT, respectively) could give rise to asymmetric strain evolution; and (3) increased relaxation occurs commensurate with the $LaAlO_3$ undergoing a cubic to rhombohedral structural phase transition at ∼450 °C[38] at which point a high density of twin defects are formed in the substrate. Transport studies reveal several similarities and differences to the trends observed in the nonstoichiometric films (Figure 3b). For both compressive ($LaAlO_3$) and tensile ($SrTiO_3$, LSAT, $NdGaO_3$) strain, we found the T_{MI} to be reduced from the bulk value of 200 K. For films grown on $LaAlO_3$ (−0.47% lattice mismatch), we note a significant stabilization of the metallic phase, with a greatly reduced $T_{MI} \approx 82$ K. Furthermore, the resistivity only changes by ∼800% from 25 to 80 K across the MIT. It is also interesting to note that films grown on $LaAlO_3$ exhibit the lowest room-temperature resistivity values (∼250 $\mu\Omega$·cm). As noted above, stoichiometric films grown on $NdGaO_3$ (1.3% tensile) exhibit an increase in resistance by 2000% over a 15 K wide temperature range about the phase transition (the onset of which occurs at ∼161 K). Films grown on LSAT (1.6% tensile) were seen to possess a $T_{MI} \approx 147$ K with a change in resistance of ∼800% between 147 and 103 K. This is drastically different form the films on $NdGaO_3$, despite possessing almost the exact same strain state. Finally, the films grown on $SrTiO_3$ (2.5% tensile) possess the sharpest transition at ∼162 K, with an increase in resistance of 6500% across the MIT.

These results for the study of epitaxial strain effects are different from those observed in nonstoichiometric samples for a number of reasons. First, increasing tensile strain was not observed to necessarily diminish the sharpness of the MIT. While we observed a broadening of the hysteresis for samples grown on LSAT, the MIT for samples grown on $SrTiO_3$ was the sharpest. Second, the value of T_{MI} was not observed to scale directly with strain, as was the case for nonstoichiometric films. Indeed, the T_{MI} values for all films grown under tensile strain were ∼150 K with no clear trend when transitioning from 1.3 to 1.6 to 2.5% lattice mismatch. Third, the overall magnitude of the transition did not have a clear trend with increasing lattice mismatch. One similarity, however, is that films with the least amount of overall strain (those grown on $LaAlO_3$) possess the lowest resistivity values. Increasing tensile strain universally leads to increased values of room-temperature resistivity. We can account for the effects of strain on the MIT based on a number of factors. Under ideal conditions, compressive strain is associated with a reduction of the Ni−O bond distance and a stabilization of the metallic phase when compared to bulk.[14] Indeed, for ultrathin films (<10 nm) grown with compressive strain, the insulating phase is suppressed entirely.[39] We can also observe an interesting effect for films grown with similar values of strain but different crystal symmetries, such as those grown on orthorhombic $NdGaO_3$ and cubic LSAT substrates. To reiterate, films grown on $NdGaO_3$ substrates exhibit sharp transitions (resistance increase of 2000% from 146 to 161 K), while films grown on LSAT substrates exhibit broaden transitions (resistance increase of 800% from 103 to 147 K). We hypothesize that the difference in symmetry in the substrates (orthorhombic for $NdGaO_3$ and cubic for LSAT) results in single-structural variant films (with either *ab*-oriented films or *c*-oriented) on $NdGaO_3$ and multistructural variant films on LSAT. In the latter, the crystallographic boundaries between the competing phases could lead to diminished transport character and ultimately causes the magnitude of the MIT to be reduced. Finally, tensile strain is associated with an expansion of the Nd−O bond, which serves to straighten the octahedral bucking angle and can stabilize the metallic phase, decreasing the T_{MI} as compared to bulk.[14] This is supported by recent studies, which have indicated that orthrorhombic nickelates, such as $NdNiO_3$, have a strong tendency to accommodate tensile strain via bond elongations.[40]

With an understanding of the effect of defect-induced strain and epitaxial strain on the MIT, we conclude by investigating a route to apply strain differently to the $NdNiO_3$ unit cell by changing the orientation of the substrate. Prior work on this topic has investigated $NdNiO_3$ on $NdGaO_3$, noting a damped MIT hysteresis for films grown on (001)- and (100)-oriented substrates.[15] This was correlated to changes in substrate strain anisotropy arising from the orthorhombic distortion of the $NdGaO_3$ substrate. To probe similar effects for a substrate without in-plane anisotropy to the lattice parameters, we grew a series of films on (001)-, (110)-, and (111)-oriented $LaAlO_3$ substrates. Films were grown to two thicknesses, 10 and 70 nm, to enable us to probe the role of thickness. X-ray diffraction

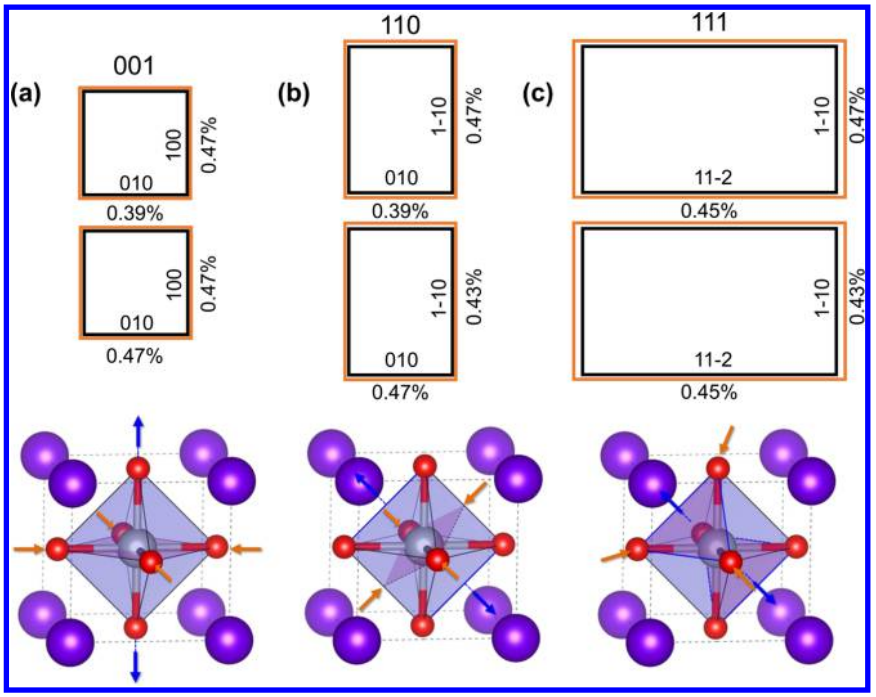

Figure 5. (Top) Schematic illustrations of the nature of in-place strain, as represented by the top orange and black polyhedral; (black) underlying $LaAlO_3$ substrate and (orange) $NdNiO_3$ film. (Bottom) Schematic illustrations of the nature of strain application on the oxygen octahedra of the system for (a) (001)-, (b) (110)-, and (c) (111)-oriented thin films. Note that the magnitude of the strain anisotropy is essentially the same, regardless of orientation, suggesting that the changes in transport are driven primarily by the nature of the strain on the octahedra.

studies of the various films reveal single-phase, epitaxial films that are coherently strained to the substrate in all cases (Supporting Information, Figures S4 and S5). Let us first begin with the resistivity profiles for these films (Figure 4a,b). The 10 nm $NdNiO_3/LaAlO_3$ (001) heterostructures (black data, Figure 4a) exhibit a sharp transition at ∼100 K, with a 100 000% change in resistivity across the MIT hysteresis. This is consistent with prior results for $NdNiO_3$ grown on $LaAlO_3$[7] and confirms the high quality of our films. On the other hand, 70 nm $NdNiO_3/LaAlO_3$ (001) heterostructures (black data, Figure 4b) exhibit slightly reduced T_{MI} and significant suppression of the magnitude of the resistivity change across the MIT. This could be due to partial relaxation effects in the film (Supporting Information, Figure S2b), as misfit and threading dislocations can induce local variations in the strain state.[41] In turn, such strain relaxation processes can broaden the MIT[42] and modify the T_{MI}.[11] In both 10 and 70 nm thick $NdNiO_3/LaAlO_3$ (001) heterostructures, however, the resistivity of the high-temperature metallic state is quite low, with values of 100−200 $\mu\Omega$·cm at 300 K.

Investigation of the transport properties of both the (110)- (blue data, Figure 4a,b) and (111)- (Figure 4a,b) oriented films, however, reveals broad transitions with very small hysteresis associated with the MIT. Focusing first on the 10 nm thick heterostructures, we observe increased resistivity for the high-temperature metallic states and the T_{MI} appears to be reduced to ∼50 and ∼70 K for (110)- and (111)-oriented heterostructures, respectively. The magnitude of the transition in both cases was greatly diminished, with resistivity changes of only ∼100% between 50 and 70 and 2 K. We observe very similar profiles for the 70 nm thick heterostructures on both (110)- and (111)-oriented substrates (Figure 4b), although the T_{MI} has shifted to ∼120 K. This could indicate relaxation effects;[11,42] although, it is interesting that, for these orientations, the T_{MI} was seen to increase with increasing thickness, while the opposite was observed for (001)-oriented heterostructures. Such results hint at a complex interplay between orientation and relaxation effects. Additionally, we remind the reader that these profiles are derived from the van der Pauw approach, which relies on roughly isotropic transport profiles along the two in-plane directions. Quick inspection of the raw, unprocessed data, however, reveals highly anisotropic transport properties along the in-plane directions of the (110)- and (111)-oriented heterostructures including changes in the T_{MI} along different directions as large as ∼60 K and differences in the resistance change below T_{MI} as large as 500%. This is not entirely unprecedented and can be seen as a result of the biaxial nature of the strain (as opposed to hydrostatic).[14] When the strain is applied diagonally to the Ni−O−Ni bond, the distortion can be expected to be different than if it were applied in-line with the Ni−O−Ni bond. This is an important consideration because when $NdNiO_3$ is grown on, for example, $LaAlO_3$ (110), the two in-plane directions are [001] and [1$\bar{1}$0]. The epitaxial strain is applied in-line with the Ni−O−Ni bond for the [001] direction but diagonally for the [1$\bar{1}$0] direction (Figure 5). Clearly, additional detailed studies of the transport along the different in-plane crystallographic directions may be necessary to fully understand the relationship between epitaxial strain and transport in these systems.

On the basis of these findings, it is clear that the transport character is highly dependent on substrate orientation. In previous work on $NdNiO_3/NdGaO_3$ heterostructures, the relationship between orientation and transport was explained by strain anisotropy.[15] We observe similar responses to changes in substrate orientation, however, and the strain values in the $NdNiO_3/LaAlO_3$ system are not especially anisotropic. We remind the reader that $NdNiO_3$ possesses an orthorhombic structure with lattice parameters a = 5.389 Å, b = 5.382 Å, and c

= 7.610 Å, while $LaAlO_3$ possesses a rhombohedral structure with a = 3.79 Å. It is unclear which orientation the orthorhombic $NdNiO_3$ structure prefers to take on $LaAlO_3$, if there is a preference at all. As a result, there are two scenarios for in-plane strain, depending on the orientation of the film unit cell direction (Figure 5). In either scenario, the strain values fall between 0.39 and 0.47% for all orientations, and the anisotropy of the two in-plane directions only decreases when transitioning to (110)- and (111)-oriented films. For this reason, the anisotropy of the strain does not seem to be the key, most important parameter. Rather, the orientation of the oxygen octahedra within the strain field appears to be of more importance. A schematic of the orientation of the octahedra for each orientation is provided (Figure 5, bottom). Note that for (001)-oriented heterostructures (Figure 5a), there is a compression along the two in-plane directions and an expansion along the out-of-plane direction. For the (110)-oriented heterostructures, on the other hand, there is a compression along one set of vertices of the octahedra, compression along one set of edges of the octahedra, and expansion along the out-of-plane octahedra edge (Figure 5b). Finally, for (111)-oriented heterostructures, there is a compression along the in-plane faces with an expansion along the out-of-plane octahedra face (Figure 5c). Given the importance of octahedral tilts and bond lengths in the $RNiO_3$ system, the orientation of the octahedra within the strain field is a highly important detail, and a theoretical precedent for this has been set in literature. Indeed, it has been previously predicted that the biaxial nature of epitaxial strain could be expected to induce anisotropy in the transport properties of the rare earth nickelate systems.[14] This, it was suggested, arises from the different buckling angles associated with the application of strain along different directions, though the net effect is not intuitive or simple to model.

CONCLUSIONS

We have demonstrated that laser fluence has a marked effect on the composition of $NdNiO_3$ films and, in turn, their physical properties. Deviations in the cation stoichiometry by up to 15% were seen to be soluble in the $NdNiO_3$ perovskite phase. Both structural and electrical properties were found to be highly sensitive to such deviations. Expansions to the out-of-plane lattice parameter were found, indicating the presence of lattice-distorting cation defects. The transport properties (as compared to stoichiometric and bulk effects) were observed to be diminished in the presence of nonstoichiometry, illustrating the importance of understanding and controlling the growth process to synthesize ideal films. Separating out the impact of extrinsic effects, we were able to conclusively determine the role that epitaxial strain plays in controlling the MIT for $NdNiO_3$. We found that both compressive and tensile strain yield T_{MI} values diminished from bulk, although films under compressive strain were found to possess lower values. Finally, we investigated the influence of substrate orientation on transport properties for the (110)- and (111)-oriented films. These results indicate the importance of understanding how the complex interplay between stoichiometry, strain, and orientation impact the structure of the oxygen octahedra and subsequent transport profiles.

ASSOCIATED CONTENT

Supporting Information

Laser optics setup; determination of laser fluence; additional X-ray diffraction studies and data for fluence and substrate effects; Rutherford backscattering spectrometry fitting; and additional X-ray diffraction data for orientation effects. This material is available free of charge via the Internet at http://pubs.acs.org.

AUTHOR INFORMATION

Corresponding Author

*E-mail: lwmartin@berkeley.edu.

Author Contributions

The manuscript was written through contributions of all authors. All authors have given approval to the final version of the manuscript. E.B. synthesized and characterized the materials. Z.C. and A.R.D. provided help with sample characterization and data analysis. L.W.M. supervised the work.

Notes

The authors declare no competing financial interest.

ACKNOWLEDGMENTS

E.B. acknowledges the support of the National Science Foundation under grant DMR-1124696. Z.H.C. acknowledges the support of the Air Force Office of Scientific Research under grant FA9550-12-1-0471. A.R.D. acknowledges support from the Army Research Office under grant W911NF-14-1-0104. L.W.M. acknowledges support from the Department of Energy under grant DE-SC0012375.

REFERENCES

(1) Koster, G.; Klein, L.; Siemons, W.; Rijnders, G.; Dodge, J. S.; Eom, C.-B.; Blank, D. H. A.; Beasley, M. R. Structure, Physical Properties, and Applications of $SrRuO_3$ Thin Films. *Rev. Mod. Phys.* **2012**, *84*, 253−298.

(2) Imada, M.; Fujimori, A.; Tokura, Y. Metal-Insulator Transitions. *Rev. Mod. Phys.* **1998**, *70*, 1039−1263.

(3) Yang, Z.; Ko, C.; Ramanathan, S. Oxide Electronics Utilizing Ultrafast Metal-Insulator Transitions. *Annu. Rev. Mater. Res.* **2011**, *41*, 337−367.

(4) Medarde, M. L. Structural, Magnetic and Electronic Properties of $RNiO_3$ Perovskites (R = Rare Earth). *J. Phys.: Condens. Matter* **1997**, *9*, 1697−1707.

(5) Sarma, D. D.; Shanthi, N.; Mahadevan, P. Electronic Structure and the Metal-Insulator Transition in $LnNiO_3$ (Ln = La, Pr, Nd, Sm, and Ho): Bandstructure Results. *J. Phys.: Condens. Matter* **1994**, *6*, 10467−10474.

(6) Balachandran, P. V.; Rondinelli, J. M. Interplay of Octahedral Rotations and Breathing Distortions in Charge-Ordering Perovskite Oxides. *Phys. Rev. B* **2013**, *88*, 054101.

(7) Scherwitzl, R.; Zubko, P.; Lesama, I. G.; Ono, S.; Morpurgo, A. F.; Catalan, G.; Triscone, J.-M. Electric-Field Control of the Metal-Insulator Transition in Ultrathin $NdNiO_3$ Films. *Adv. Mater.* **2010**, *22*, 5517−5520.

(8) Kiri, P.; Hyett, G.; Binions, R. Solid State Thermochromic Materials. *Adv. Mater. Lett.* **2010**, *1*, 86−105.

(9) Obrandors, X.; Paulius, L. M.; Maple, M. B.; Torrance, J. B.; Nazzal, A. I.; Fontcuberta, J.; Granados, X. Pressure Dependence of the Metal-Insulator Transition in the Charge-Transfer Oxides $RNiO_3$ (R = Pr, Nd, $Nd_{0.7}La_{0.3}$). *Phys. Rev. B* **1993**, *47*, 12353.

(10) Canfield, P. C.; Thompson, J. D.; Cheong, S. W.; Rupp, L. W. Extraordinary Pressure Dependence of the Metal-to-Insulator Transition in the Charge-Transfer Compounds $NdNiO_3$ and $PrNiO_3$. *Phys. Rev. B* **1993**, *47*, 12357.

(11) Tiwari, A.; Jin, C.; Narayan, J. Strain-Induced Tuning of Metal-Insulator Transition in $NdNiO_3$. *Appl. Phys. Lett.* **2002**, *80*, 4039−4041.
(12) Liu, J.; Kareev, M.; Gray, B.; Kim, J. W.; Ryan, P.; Dabrowski, B.; Freeland, J. W.; Chakhalian, J. Strain-Mediated Metal-Insulator Transition in Epitaxial Ultrathin Films of $NdNiO_3$. *Appl. Phys. Lett.* **2010**, *96*, 233110.
(13) Garcia-Munoz, J. L.; Suaaidi, M.; Martinez-Lope, M. J.; Alonso, J. A. Influence of Carrier Injection on the Metal-Insulator Transition in Electron- and Hole-Doped $R_{1-x}A_xNiO_3$ Perovskites. *Phys. Rev. B* **1995**, *52*, 13563.
(14) Catalan, G. Progress in Perovskite Nickelate Research. *Phase Transitions* **2008**, *81*, 729−749.
(15) Lian, X. K.; Chen, F.; Tan, K. L.; Chen, P. F.; Wang, L. F.; Gao, G. Y.; Jin, S. W.; Wu, W. B. Anisotropic-Strain-Controlled Metal-Insulator Transition in Epitaxial $NdNiO_3$ Films Grown on Orthorhombic $NdGaO_3$ Substrates. *Appl. Phys. Lett.* **2013**, *103*, 172110.
(16) May, S. J.; Kim, J.-W.; Rondinelli, J. M.; Karapetrova, E.; Spaldin, N. A.; Bhattacharya, A.; Ryan, P. J. Quantifying Octahedral Rotations in Strained Perovskite Oxide Films. *Phys. Rev. B* **2010**, *82*, 014110.
(17) Bruno, F. Y.; Rushchanskii, K. Z.; Valencia, S.; Dumont, Y.; Carretero, C.; Jacquet, E.; Abrudan, R.; Blugel, S.; Lezaic, M.; Bibes, M.; Barthelemy, A. Rationalizing Strain Engineering Effects in Rare-Earth Nickelates. *Phys. Rev. B* **2013**, *88*, 195108.
(18) Tiwari, A.; Rajeev, K. P. Effect of Oxygen Stoichiometry on the Electrical Resistivity Behaviour of $NdNiO_{3-\delta}$. *Solid State Commun.* **1999**, *109*, 119−124.
(19) Nikulin, I. V.; Novojilov, M. A.; Kaul, A. R.; Mudretsova, S. N.; Kondrashov, S. V. Oxygen Nonstoichiometry of $NdNiO_{3-\delta}$ and $SmNiO_{3-\delta}$. *Mater. Res. Bull.* **2004**, *39*, 775−791.
(20) Qiao, L.; Droubay, T. C.; Shutthanandan, V.; Zhu, Z.; Sushko, P. V.; Chambers, S. A. Thermodynamic Instability at the Stoichiometric $LaAlO_3/SrTiO_3$ (001) Interface. *J. Phys.: Condens. Matter* **2010**, *22*, 312201.
(21) Droubay, T. C.; Qiao, L.; Kaspar, T. C.; Engelhard, M. H.; Shutthanandan, V.; Chambers, S. A. Nonstoichiometric Material Transfer in the Pulsed Laser Deposition of $LaAlO_3$. *Appl. Phys. Lett.* **2010**, *97*, 124105.
(22) Ohnishi, T.; Lippmaa, M.; Yamamoto, T.; Meguro, S.; Koinuma, H. Improved Stoichiometry and Misfit Control in Perovskite Thin Film Formation at a Critical Fluence by Pulsed Laser Deposition. *Appl. Phys. Lett.* **2005**, *87*, 241919.
(23) Ohnishi, T.; Shibuya, K.; Yamamoto, T.; Lippmaa, M. Defects and Transport in Complex Oxide Thin Films. *J. Appl. Phys.* **2008**, *103*, 103703.
(24) Breckenfeld, E.; Wilson, R.; Karthik, J.; Damodaran, A. R.; Cahill, D. G.; Martin, L. W. Effect of Growth Induced (Non)-Stoichiometry on the Structure, Dielectric Response, and Thermal Conductivity of $SrTiO_3$ Thin Films. *Chem. Mater.* **2012**, *24*, 331−337.
(25) Breckenfeld, E.; Wilson, R. B.; Martin, L. W. Effect of Growth Induced (Non)Stoichiometric on the Thermal Conductivity, Permittivity, and Dielectric Loss of $LaAlO_3$ Films. *Appl. Phys. Lett.* **2013**, *103*, 082901.
(26) Breckenfeld, E.; Shah, A. B.; Martin, L. W. Strain Evolution in Non-Stoichiometric Heteroepitaxial Thin Film Perovskites. *J. Mater. Chem. C* **2013**, *1*, 8052−8059.
(27) Breckenfeld, E.; Shah, A. B.; Martin, L. W. Strain Evolution in Non-Stoichiometric Heteroepitaxial Thin Film Perovskites. *J. Mater. Chem. C* **2013**, *1*, 8052−8059.
(28) Catalan, G.; Bowman, R. M.; Gregg, J. M. Transport Properties of $NdNiO_3$ Thin Films made by Pulsed-Laser Deposition. *J. Appl. Phys.* **2000**, *87*, 606−608.
(29) Kaur, D.; Jesudasan, J.; Raychaudhuri, P. Pulsed Laser Deposition of $NdNiO_3$ Thin Films. *Solid State Commun.* **2005**, *136*, 369−374.
(30) Breckenfeld, E.; Bronn, N.; Karthik, J.; Damodaran, A. R.; Lee, S.; Mason, N.; Martin, L. W. Effect of Growth Induced (Non)-Stoichiometry on Interfacial Conductance in $LaAlO_3/SrTiO_3$. *Phys. Rev. Lett.* **2013**, *110*, 196804.
(31) Warusawithana, M. P.; Richter, C.; Mundy, J. A.; Roy, P.; Ludwig, J.; Paetel, S.; Heeg, T.; Pawlicki, A. A.; Kourkoutis, L. F.; Zheng, M.; Lee, M.; Mulchay, B.; Zander, W.; Zhu, Y.; Schubert, J.; Eckstein, J. N.; Muller, D. A.; Hellberg, C. S.; Mannhart, J.; Schlom, D. G. $LaAlO_3$ Stoichiometry is key to Electron Liquid Formation at $LaAlO_3/SrTiO_3$ Interfaces. *Nat. Commun.* **2013**, *4*, 2351.
(32) Sato, H. K.; Bell, C.; Hikita, Y.; Hwang, H. W. Stoichiometry Control of the Electronic Properties of the $LaAlO_3/SrTiO_3$ Heterointerfaces. *Appl. Phys. Lett.* **2013**, *102*, 251602.
(33) Breckenfeld, E.; Bronn, N.; Mason, N.; Martin, L. W. Tunability of Conduction at the $LaAlO_3/SrTiO_3$ Heterointerface: Thickness and Compositional Studies. *Appl. Phys. Lett.* **2014**, *105*, 121610.
(34) Retoux, R.; Rodriguez-Carvajal, R.; Lacorre, P. Neutron Diffraction and TEM Studies of the Crystal Structure and Defects of $Nd_4Ni_3O_8$. *J. Solid State Chem.* **1998**, *140*, 307−315.
(35) Scherwitzl, R. Metal-insulator transitions in nickelate heterostructures. Doctoral Dissertation, University of Geneva, Geneva, Switzerland, 2012.
(36) Kalinin, S. V.; Borisevich, A.; Fong, D. Beyond Condensed Matter Physics on the Nanoscale: The Role of Ionic and Electrochemical Phenomena in the Physical Functionalities of Oxide Materials. *ACS Nano* **2012**, *6*, 10423−10437.
(37) Liu, X.; Prasad, A.; Nishio, J.; Weber, E. R.; Liliental-Weber, Z.; Walukiewicz, W. Native Point Defects in Low-Temperature Grown GaAs. *Appl. Phys. Lett.* **1995**, *67*, 279−281.
(38) Hayward, S. A.; Morrison, F. D.; Redfern, S. A. T.; Salje, E. K. H.; Scott, J. F.; Knight, K. S.; Tarantino, S.; Glazer, A. M.; Shuvaeva, V.; Daniel, P.; Zhang, M.; Carpenter, M. A. Transformation Processes in $LaAlO_3$: Neutron Diffraction, Dielectric, Thermal, Optical, and Raman Studies. *Phys. Rev. B* **2005**, *72*, 054110.
(39) Liu, J.; Kargarian, M.; Kareev, M.; Gray, B.; Ryan, P. J.; Crux, A.; Tahir, N.; Chuang, Y.-D.; Guo, J.; Rondinelli, J. M.; Freeland, J. W.; Fiete, G. A.; Chakhalian, J. Heterointerface Engineered Electronic and magnetic Phases of $NdNiO_3$ Thin Films. *Nat. Commun.* **2013**, *4*, 2714.
(40) Tung, I. C.; Balachandran, P. V.; Liu, J.; Bray, B. A.; Karapetrova, E. A.; Lee, J. H.; Chakhalian, J.; Bedzyk, M. J.; Rondinelli, J. M.; Freeland, J. W. Connecting Bulk Symmetry and Orbital Polarization in Strained $RNiO_3$ Ultrathin Films. *Phys. Rev. B* **2013**, *88*, 205112.
(41) Benia, H.-M.; Myrach, P.; Gonchar, A.; Risse, T.; Nilius, N.; Freund, H.-J. Electron Trapping in Misfit Dislocations of MgO Thin Films. *Phys. Rev. B* **2010**, *81*, 241415.
(42) Kumar, D.; Rajeev, K. P.; Kushwaha, A. K.; Budhani, R. C. Heterogeneous Nucleation and Metal-Insulator Transition in Epitaxial Films of $NdNiO_3$. *J. Appl. Phys.* **2010**, *108*, 063503.